

A Comparison Study of the Effects of Ba and La Doping in Sr_2IrO_4 : Ir–O–Ir Bond Angle and Carrier Concentration

Tao Han¹ · Dandan Liang¹ · Yongjian Wang¹ · Jun Yang¹ · Hui Han¹ ·
Jingrong Wang¹ · Jixiang Gong¹ · Lei Luo¹ · W. K. Zhu¹ · Changjin Zhang¹ ·
Yuheng Zhang¹

Received: 7 March 2017 / Accepted: 28 April 2017
© Springer Science+Business Media New York 2017

Abstract We perform a systematic investigation on the effects of Ba and La doping on the lattice and transport properties of Sr_2IrO_4 , which is theoretically predicted to be a host compound of high-temperature superconductivity. We observe a drastic straightening of the Ir–O–Ir bond angle in the Ba-doped samples. The straightening of the bond angle is much weaker in the La-doped samples. It is found that the La doping leads to the introduction of electron-type charge carriers, while the charge carrier concentration does not change too much in the Ba-doped samples. As a result, both the resistivity and the magnetic moments decrease much faster in the La-doped samples, compared to those in the Ba-doped samples. The present results suggest that it is the charge carrier density rather than the Ir–O–Ir bond angle that dominates the magnetic and transport properties of the Sr_2IrO_4 system.

Keywords High-temperature superconductivity · Ir–O–Ir bond angle · Charge carrier concentration · Sr_2IrO_4

1 Introduction

Recently, $5d$ transition metal oxide Sr_2IrO_4 with layered perovskite structure has attracted intensive attention as a

candidate for a novel Mott insulator [1–10]. Sr_2IrO_4 forms in a reduced tetragonal $I4_1/acd$ structure, similar to the tetragonal $I4/mmm$ structure in isostructural La_2CuO_4 but with the Ir–O–Ir bond angle being significantly bended. Considering its odd number of electrons per unit formula ($5d^5$) and the highly delocalized $5d$ electronic orbitals of the Ir ions, one expects a metallic state in a naive band picture. However, the Sr_2IrO_4 is unexpectedly found to be an insulator. The insulating behavior has been attributed to the strong spin-orbit coupling ($\zeta_{\text{SO}} \sim 0.4$ eV) which is comparable to the Coulomb repulsion $U = 0.5 \sim 2$ eV, giving rise to a novel $J_{\text{eff}} = 1/2$ Mott-insulating ground state [1].

Taking into account the facts that Sr_2IrO_4 has a similar crystal lattice structure and the same Mott-insulating ground state with the high-temperature superconducting cuprate parent compound La_2CuO_4 , it has been proposed that the novel superconducting phase can be expected when carriers are properly doped in this compound [11–15]. As a matter of fact, angle-resolved photoemission spectra of Sr_2IrO_4 reveal the existence of disconnected segments of zero-energy states, known as Fermi arcs, with a gap as large as 80 meV [16–18]. The occurrence of Fermi arcs in Sr_2IrO_4 is of particular importance for investigating possible unconventional superconductivity: it is still strongly controversial whether the Fermi arcs are a precursor signature of d -wave superconductivity. Different from the $\text{La}_{2-x}\text{Sr}_x\text{CuO}_4$ and $\text{La}_{2-x}\text{Ba}_x\text{CuO}_4$ where only a few percent of doping at the La site leads to a metal-insulator transition and superconductivity, the insulating phase in the Sr_2IrO_4 compound is very robust against Sr-site doping or application of high pressure [19–22].

Comparing to the nearly straightened Cu–O–Cu bond angle in La_2CuO_4 , the Ir–O–Ir bond angle in Sr_2IrO_4 is greatly bended. As is well known, the conductance in K_2NiF_4 -type compounds is quasi-two-dimensional. Thus, it is reasonable

✉ W. K. Zhu
wkzhu@hmfl.ac.cn

✉ Changjin Zhang
zhangcj@hmfl.ac.cn

¹ High Magnetic Field Laboratory, Chinese Academy of Sciences and University of Science and Technology of China, Hefei 230031, China

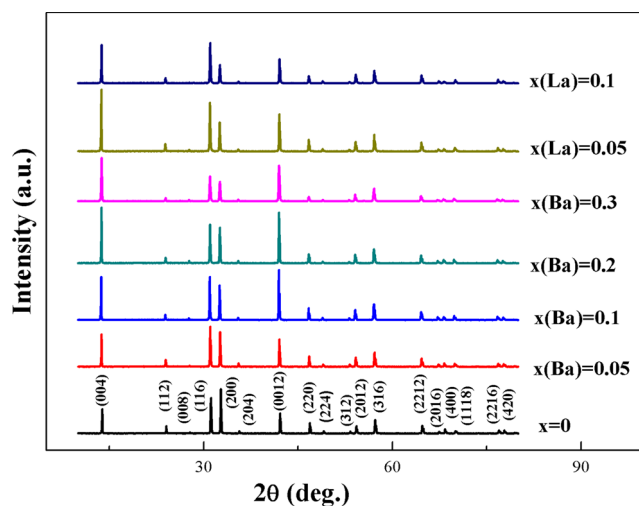


Fig. 1 Powder XRD patterns of $\text{Sr}_{2-x}\text{Ba}_x\text{IrO}_4$ ($x = 0, 0.05, 0.1, 0.2,$ and 0.3) and $\text{Sr}_{2-x}\text{La}_x\text{IrO}_4$ ($x = 0.05$ and 0.1) samples

to conclude that the Ir–O–Ir bond angle could play an important role in the robustness of the insulating state. However, to our best knowledge, there is very little study on the role of the Ir–O–Ir bond angle in the Sr_2IrO_4 compound.

In this work, we perform a comparison investigation on the influence of the Ir–O–Ir bond angle and the transport and magnetic properties of two series of Ba- and La-doped Sr_2IrO_4 samples. It is found that the Ba doping in Sr_2IrO_4 indeed leads to straightening of the Ir–O–Ir bond angle, while the La doping alters the Ir–O–Ir bond angle very little. However, from the transport and magnetic data, we find that comparing to the Ba doping case, the La doping results in a much enhanced conductance and a decreased magnetic moment of the samples. The present results suggest that the Ir–O–Ir bond angle plays a relatively less important role in the conductance and magnetic properties of the Sr_2IrO_4 compound.

2 Materials and Methods

Polycrystalline samples of $\text{Sr}_{2-x}\text{Ba}_x\text{IrO}_4$ ($x = 0, 0.05, 0.1, 0.2,$ and 0.3) and $\text{Sr}_{2-x}\text{La}_x\text{IrO}_4$ ($x = 0.05$ and 0.1)

Table 1 Structural parameters and Hall coefficients of $\text{Sr}_{2-x}\text{Ba}_x\text{IrO}_4$ ($x = 0, 0.05, 0.1, 0.2,$ and 0.3) and $\text{Sr}_{2-x}\text{La}_x\text{IrO}_4$ ($x = 0.05$ and 0.1) samples at 300 K

Sample	a (Å)	c (Å)	Ir–O–Ir bond angle (°)	R_H ($\text{cm}^3 \text{C}^{-1}$)	n_H (cm^{-3})
$x = 0$	5.4941	25.8036	157.3	340	$1.84 * 10^{16}$
x (Ba) = 0.05	5.4955	25.8096	157.9	36.1	$1.74 * 10^{17}$
x (Ba) = 0.1	5.4960	25.8141	163.4	60	$1.04 * 10^{17}$
x (Ba) = 0.2	5.5016	25.8353	172.1	102	$6.11 * 10^{16}$
x (Ba) = 0.3	5.5060	25.8491	178.3	15.1	$4.14 * 10^{17}$
x (La) = 0.05	5.4993	25.7854	157.5	−16.67	$-3.75 * 10^{17}$
x (La) = 0.1	5.5026	25.7824	159.1	−9.55	$-6.54 * 10^{17}$

were prepared by conventional solid-state reaction method. Stoichiometric powders of SrCO_3 (99.9%), IrO_2 (99.9%), BaCO_3 (99.9%), and La_2O_3 (99.9%) were mixed, ground, and heated at 1050 °C for 1 day, followed by several times of calcining at 1250 °C for 2 days. The crystal structure and phase purity were checked by powder X-ray diffraction (XRD) on a Rigaku-TTR3 X-ray diffractometer using $\text{Cu K}\alpha$ radiation. Rietveld refinement was performed for XRD data using the GSAS software package. The resistivity was taken on a Sumitomo CNA-11 cryogenic system, Hall effect measurements were taken on an Oxford TeslatronPT cryogenic system, and the magnetic measurements were taken on a Quantum Design SQUID-VSM3.

3 Results and Discussion

Figure 1 shows the powder XRD patterns of $\text{Sr}_{2-x}\text{Ba}_x\text{IrO}_4$ ($x = 0, 0.05, 0.1, 0.2,$ and 0.3) and $\text{Sr}_{2-x}\text{La}_x\text{IrO}_4$ ($x = 0.05$ and 0.1) samples at room temperature. All the peaks can be indexed with the space group $I4_1/acd$. In order to check the change of lattice constants and Ir–O–Ir bond angles, the refinements of XRD data are further performed. As shown in Table 1, the Ba doping increases the lattice constants of both a and c , and straightens the Ir–O–Ir bond angle. The calculated parameters of $\text{Sr}_{2-x}\text{Ba}_x\text{IrO}_4$ ($x = 0.3$) are $a = 5.5060$ Å and $c = 25.8491$ Å, which are both larger than those of the undoped Sr_2IrO_4 , i.e., $a = 5.4941$ Å and $c = 25.8026$ Å. The enlargement of the lattice constants in the Ba-doped samples is consistent with the fact that the ionic radius of Ba^{2+} is larger than that of Sr^{2+} . The Ir–O–Ir bond angle is increased from 157.3° for Sr_2IrO_4 to 178.3° for $\text{Sr}_{2-x}\text{Ba}_x\text{IrO}_4$ ($x = 0.3$). On the other hand, La doping decreases the c parameter. The lattice parameters of $\text{Sr}_{2-x}\text{La}_x\text{IrO}_4$ ($x = 0.1$) are $a = 5.5026$ Å and $c = 25.7826$ Å. The Ir–O–Ir bond angle of $\text{Sr}_{2-x}\text{La}_x\text{IrO}_4$ ($x = 0.1$) is 159.1°, which is only slightly larger than that of the undoped sample.

Figure 2 shows the temperature dependence of the electrical resistivity for the $\text{Sr}_{2-x}\text{Ba}_x\text{IrO}_4$ ($x = 0, 0.05, 0.1, 0.2,$ and 0.3) and $\text{Sr}_{2-x}\text{La}_x\text{IrO}_4$ ($x = 0.05$ and 0.1) samples. All the samples exhibit an insulating behavior from

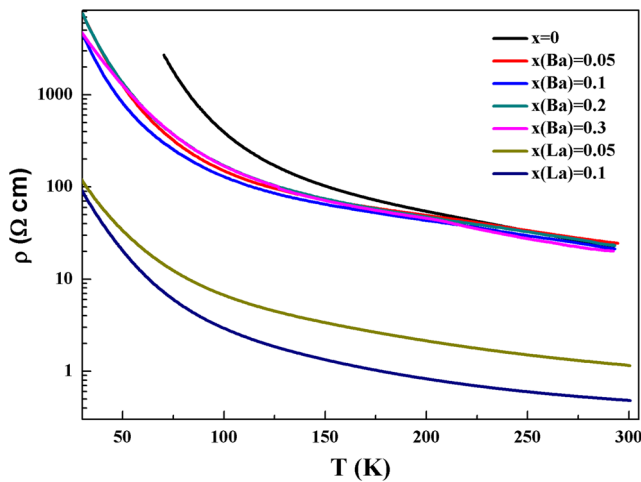


Fig. 2 Temperature dependence of resistivity of $\text{Sr}_{2-x}\text{Ba}_x\text{IrO}_4$ ($x = 0, 0.05, 0.1, 0.2,$ and 0.3) and $\text{Sr}_{2-x}\text{La}_x\text{IrO}_4$ ($x = 0.05$ and 0.1) samples

room temperature down to low temperature. The Ba doping seems to induce little change in the insulating nature, despite the fact that the Ir–O–Ir bond angle is significantly straightened. Differently, the La doping greatly decreases the electrical resistivity. For instance, the room-temperature resistivity decreases from about $20 \text{ } \Omega\text{cm}$ for $\text{Sr}_{2-x}\text{Ba}_x\text{IrO}_4$ ($x = 0, 0.05, 0.1, 0.2,$ and 0.3) to $1.15 \text{ } \Omega\text{cm}$ for $x(\text{La}) = 0.05$ sample and further to $0.5 \text{ } \Omega\text{cm}$ for $x(\text{La}) = 0.1$ sample.

In order to better understand the changes in resistivity, Hall resistivity measurements were carried out at 300 K. As shown in Table 1, the calculated Hall coefficient R_H of $\text{Sr}_{2-x}\text{Ba}_x\text{IrO}_4$ ($x = 0, 0.05, 0.1, 0.2,$ and 0.3) samples at room temperature are all positive, implying that their dominant carriers are holes. However, R_H turns into negative when a small proportion of La is introduced, showing an electron-dominant nature for $\text{Sr}_{2-x}\text{La}_x\text{IrO}_4$ ($x = 0.05$ and 0.1) samples. Moreover, the carrier concentration n_H changes from $1.84 \times 10^{16} \text{ cm}^{-3}$ for Sr_2IrO_4 to $-3.75 \times 10^{17} \text{ cm}^{-3}$ for $x(\text{La}) = 0.05$ sample and further to $-6.54 \times 10^{17} \text{ cm}^{-3}$ for $x(\text{La}) = 0.1$ sample. These facts suggest that effective electron carriers are substantially introduced in La-doped samples, which leads to the greatly decreased resistivity. This is consistent with previous researches [23]. It is also reasonable that the Ba doping does not affect the electrical transport too much, since it does not apparently change the carrier type and carrier concentration.

According to previous researches [23–25], the chemical doping at the A site influences both the electrical transport and the magnetic properties. Figure 3 presents the field cooling magnetizations as a function of temperature taken at a field of 5000 Oe for both the undoped and doped samples. All the curves show a ferromagnetic-like behavior at low temperature. Actually, the magnetic ground state of

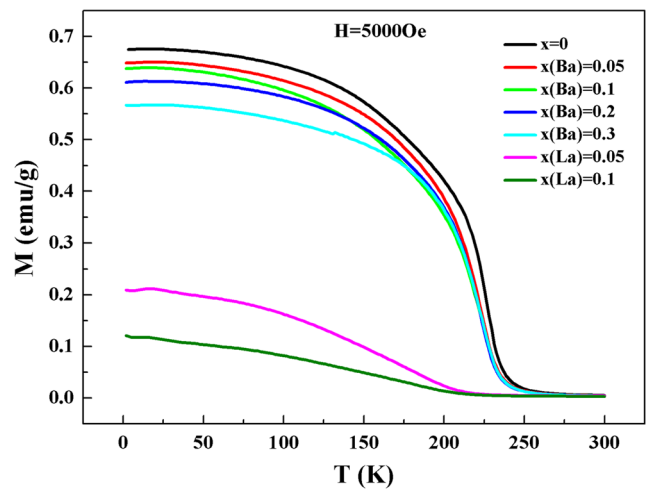


Fig. 3 Temperature dependence of field cooling magnetizations taken at a field of 5000 Oe for $\text{Sr}_{2-x}\text{Ba}_x\text{IrO}_4$ ($x = 0, 0.05, 0.1, 0.2,$ and 0.3) and $\text{Sr}_{2-x}\text{La}_x\text{IrO}_4$ ($x = 0.05$ and 0.1) samples from 1.8 to 300 K

the Sr_2IrO_4 parent compound is canted antiferromagnetism with a net moment of $0.06 \mu_B/\text{Ir}$ [26, 27]. The transition temperature T_C stays at 240 K for $\text{Sr}_{2-x}\text{Ba}_x\text{IrO}_4$ ($x = 0, 0.05, 0.1, 0.2,$ and 0.3) samples and decreases to 210 K for $\text{Sr}_{2-x}\text{La}_x\text{IrO}_4$ ($x = 0.05$ and 0.1) samples. Similar to the change of transition temperature, the decrease of the saturated moment in La-doped samples is much larger than that in Ba-doped samples. As La doping offers electrons and turns Ir^{4+} ions into Ir^{3+} ions ($5d^6$), which do not possess an uncompensated moment in the $J_{\text{eff}} = 1/2$ picture, the overall magnetic moment is thus reduced and the exchange interactions (i.e., transition temperature) are weakened in the La-doped samples.

In order to understand the magnetic ground states in these samples, the magnetization vs. magnetic field (M - H) measurements are further performed. Figure 4 shows the M - H

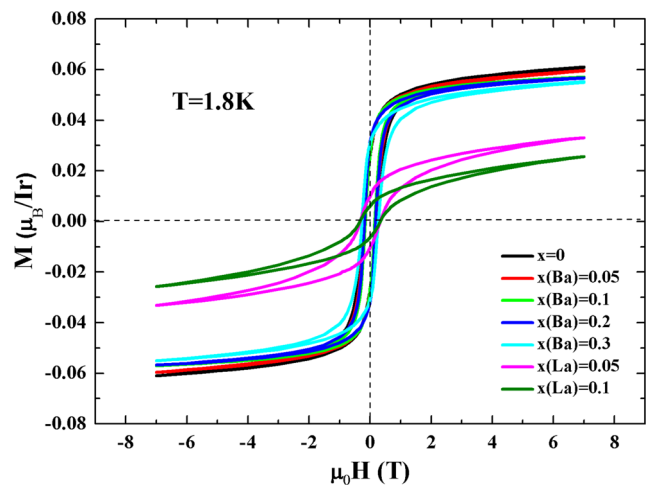


Fig. 4 Magnetization vs. magnetic field at 1.8 K in the field range of $\pm 7 \text{ T}$

curves taken at 1.8 K. The hysteresis loops, with a linear-like increase in magnetization at high fields, indicate a canted antiferromagnetic ground state. Both the Ba doping and La doping do not change the magnetic ground state. However, the doping results in a reduction of saturated moment M_S in both systems. The M_S decreases more quickly in $\text{Sr}_{2-x}\text{La}_x\text{IrO}_4$ than in $\text{Sr}_{2-x}\text{Ba}_x\text{IrO}_4$, i.e., $0.055 \mu_B/\text{Ir}$ for Sr_2IrO_4 , $0.048 \mu_B/\text{Ir}$ for x (Ba) = 0.3 sample, and $0.016 \mu_B/\text{Ir}$ for x (La) = 0.1 sample. All the saturated moments are calculated after subtracting the linear antiferromagnetic part.

The much more decrease in both the resistivity and the magnetic moment in La-doped samples than that in Ba-doped samples could be due to the difference in the valance states. Though the isovalent Ba doping straightens the Ir–O–Ir bond angle, it does little change to the carrier type and low carrier concentration which plays an important role in the electrical transport. By combining the electrical and magnetic measurements, we could find that the straightened Ir–O–Ir bond angle by Ba doping does not give rise to any significant changes in either electrical conductance or magnetic properties. In contrast, the doped electrons and Ir^{3+} ions caused by La doping are responsible for both the enhanced electrical conductance and the decreased magnetic moment and transition.

4 Conclusion

In conclusion, we have synthesized two series of Ba- and La-doped Sr_2IrO_4 samples and investigated their lattice structure, magnetic, and transport properties. The Ba doping leads to significant straightening of the Ir–O–Ir bond angle while it does not introduce too much extra charge carriers. On the other hand, the La doping has less influence on the Ir–O–Ir bond angle but it efficiently introduces electron charge carriers into the Sr_2IrO_4 compound. Accordingly, the La doping in the Sr_2IrO_4 system results in an enhanced conductance and a reduced magnetic moment compared with those in Ba-doped samples. The present results suggest that the bended Ir–O–Ir bond angle plays a less important role in the robustness of the insulating state. The insulating ground state cannot be changed by the mere regulation of the Ir–O–Ir bond angle. The introduction of efficient charge carriers is the reason for the enhanced conductance and the reduced magnetic moment.

Acknowledgments This work was supported by the National Key Research and Development Program of China (Grant No. 2016YFA0300404), the National Natural Science Foundation of China (Grant Nos. U1532267, 51603207, 11674327 and 11504379), and the CASHIPS Director's Fund (Grant No. YZJJ201516). T. Han and D.D. Liang contributed equally to this paper.

References

- Kim, B.J., Jin, H., Moon, S.J., Kim, J.Y., Park, B.G., Leem, C.S., Yu, J., Noh, T.W., Kim, C., Oh, S.J., Park, J.H., Durairaj, V., Cao, G., Rotenberg, E.: *Phys. Rev. Lett.* **101**, 076402 (2008)
- Kim, B.J., Ohsumi, H., Komesu, T., Sakai, S., Morita, T., Takagi, H., Arima, T.: *Science* **323**, 1329 (2009)
- Qi, T.F., Korneta, O.B., Chikara, S., Ge, M., Parkin, S., De Long, L.E., Schlottmann, P., Cao, G.: *J. Appl. Phys.* **109**, 07D906 (2011)
- Fujiyama, S., Ohsumi, H., Komesu, T., Matsuno, J., Kim, B.J., Takata, M., Arima, T., Takagi, H.: *Phys. Rev. Lett.* **108**, 247212 (2012)
- Carter, J.M., V, V.S., Kee, H.Y.: *Phys. Rev. B* **88**, 035111 (2013)
- Nichols, J., Ali, N.B., Ansary, A., Cao, G., Ng, K.W.: *Phys. Rev. B* **89**, 085125 (2014)
- Watanabe, H., Shirakawa, T., Yunoki, S.: *Phys. Rev. B* **89**, 165115 (2014)
- Wang, C., Seinige, H., Cao, G., Zhou, J.S., Goodenough, J.B., Tsoi, M.: *Phys. Rev. B* **92**, 115136 (2015)
- Hogan, T., Yamani, Z., Walkup, D., Chen, X., Dally, R., Ward, T.Z., Dean, M.P.M., Hill, J., Islam, Z., Madhavan, V., Wilson, S.D.: *Phys. Rev. Lett.* **114**, 257203 (2015)
- Torre, A.D., Walker, S.M., Bruno, F.Y., Ricco, S., Wang, Z., Lezama, I.G., Scheerer, G., Gariat, G., Jaccard, D., Berthod, C., Kim, T.K., Hoesch, M., Hunter, E.C., Perry, R.S., Tamai, A., Baumberger, F.: *Phys. Rev. Lett.* **115**, 176402 (2015)
- Wang, F., Senthil, T.: *Phys. Rev. Lett.* **106**, 136402 (2011)
- Watanabe, H., Shirakawa, T., Yunoki, S.: *Phys. Rev. Lett.* **110**, 027002 (2013)
- Meng, Z.Y., Kim, Y.B., Kee, H.Y.: *Phys. Rev. Lett.* **113**, 177003 (2014)
- Yang, Y., Wang, W.S., Liu, J.G., Chen, H., Dai, J.H., Wang, Q.H.: *Phys. Rev. B* **89**, 094518 (2014)
- Gao, Y., Zhou, T., Huang, H.X., Wang, Q.H.: *Sci. Rep.* **5**, 09251 (2015)
- Kim, Y.K., Krupin, O., Denlinger, J.D., Bostwick, A., Rotenberg, E., Zhao, Q., Mitchell, J.F., Allen, J.W., Kim, B.J.: *Science* **345**, 187 (2014)
- Kim, Y.K., Sung, N.H., Denlinger, J.D., Kim, B.J.: *Nat. Phys.* **12**, 37 (2016)
- Zhao, L., Torchinsky, D.H., Chu, H., Ivanov, V., Lifshitz, R., Flint, R., Qi, T., Cao, G., Hsieh, D.: *Nat. Phys.* **12**, 32 (2016)
- Dong, S.T., Zhang, B.B., Zhang, L.Y., Chen, Y.B., Zhou, J., Zhang, S.T., Gu, Z.B., Yao, S.H., Chen, Y.F.: *Phys. Lett. A* **378**, 2777 (2014)
- Chen, X., Hogan, T., Walkup, D., Zhou, W., Pokharel, M., Yao, M., Tian, W., Ward, T.Z., Zhao, Y., Parshall, D., Opeil, C., Lynn, J.W., Madhavan, V., Wilson, S.D.: *Phys. Rev. B* **92**, 075125 (2015)
- Kong, J., Liu, S.L., Cheng, J., Wang, H., Li, X., Wang, Z.H.: *Solid State Commun.* **220**, 39 (2015)
- Zocco, D.A., Hamlin, J.J., White, B.D., Kim, B.J., Jeffries, J.R., Weir, S.T., Vohra, Y.K., Allen, J.W., Maple, M.B.: *J. Phys.: Condens. Matter* **26**, 255603 (2014)
- Han, T., Wang, Y.J., Yang, J., He, L., Xu, J.M., Liang, D.D., Han, H., Ge, M., Xi, C.Y., Zhu, W.K., Zhang, C.J., Zhang, Y.H.: *Appl. Phys. Lett.* **109**, 192409 (2016)
- Zhu, W.K., Wang, M., Seradjeh, B., Yang, F.Y., Zhang, S.X.: *Phys. Rev. B* **90**, 054419 (2014)
- Zhu, W.K., Lu, C.K., Tong, W., Wang, J.M., Zhou, H.D., Zhang, S.X.: *Phys. Rev. B* **91**, 144408 (2015)
- Crawford, M., Subramanian, M., Harlow, R., Baca, J.F., Wang, Z., Johnston, D.: *Phys. Rev. B* **49**, 9198 (1994)
- Kini, N.S., Strydom, A.M., Jeevan, H.S., Geibel, C., Ramakrishnan, S.: *J. Phys.: Condens. Matter* **18**, 8205 (2006)